SUPPLEMENTAL MATERIAL

Supplemental methods

Animals and experimental design

All experiments were approved by the Landesamt für Gesundheit und Soziales and conducted in accordance with the German Animal Welfare Act. Twenty-four male C57/BL6 J mice (8 weeks of age, Charles River, Germany) were housed in a temperature (22 ± 2 °C), humidity (55 ± 10 %), and light (12/12 hr light/dark cycle) controlled environment. Animals were food and water restricted for approximately 5 months whilst being trained in 9-hole boxes. Unexpectedly, one animal needed to be humanely euthanized prior to randomization in accordance with our animal permissions due to ill-health and substantial weight-loss. Bias was reduced using a pre-generated sequence to randomize the order of the surgical procedures, and with a coin to assign mice between 9-13 months of age to undergo hypoperfusion (n=12), or the corresponding sham procedure (n=11). Sample size calculations were not performed as there was no available information regarding aged mice for the hypoperfusion procedure, however, group sizes were in line with previous literature in young animals. All experimenters were blind to the condition of the animals during testing and scanning and all analysis was performed in a blinded fashion. Mice were imaged repetitively (prior to and at 24 hrs, and 1 and 4 weeks post surgery) for quantitative estimation of cerebral blood flow (CBF). DTI, magnetic resonance spectroscopy (MRS), and angiography were acquired between 5-7 weeks post surgery. The novel object recognition (NOR) test was conducted one week prior to, and between 4-5 weeks post surgery. At 6 weeks, the animals were trained in a standard hidden platform (place) task in the Morris water maze and tissue was subsequently processed for immunohistochemistry.

Hypoperfusion via bilateral common carotid artery stenosis

Anaesthesia was achieved using isoflurane in a 70:30 nitrous oxide:oxygen mixture and core body temperature was maintained at 37 ± 0.2 °C with an automated rectal probe and heat blanket. A midline incision was made in the neck, and a carotid artery was carefully exposed. Hypoperfusion was induced by winding a custom ordered, non-magnetic, surgical grade microcoil (160 μm inner diameter, Shannon Coiled Springs Microcoil, Limerick, Ireland) around one of the carotid arteries. The sham procedure was performed with a larger diameter microcoil (500 μm) that did not constrict the vessel. The muscle and glands were guided back into place and local anaesthetic was applied to the sutured wound prior to recovery. Twenty- four hours later, the same procedure was repeated on the other carotid artery. This delay represents an important refinement that does not result in higher mortality when using the smaller sized microcoils. Regular diet was placed on the floor of the cage to assist with feeding, and animals were provided with 6 mg/mL of Paracetamol in the drinking water to assist with post-operative pain (one day prior to, and up to three days post-surgery). A tumor was discovered in 1 sham animal (subsequently excluded) (sham (n=10)). One hypoperfused animal was euthanized immediately after surgery (hypoperfused (n=11)). One sham animal died during DTI acquisition, and did not undergo spectroscopy, angiography, or behavioural testing (sham (n=9).

MRI measurements

Anaesthesia was again achieved using isoflurane as per above, and body temperature and respiration rate were monitored with MRI compatible equipment (Small Animal Instruments, Inc., Stony Brook, NY).

Cerebral blood flow and angiography

CBF and angiography were measured on a 7 T Pharmascan using Paravision 5.1 software (Bruker BioSpin, Ettlingen, Germany). For the CBF measurement, radio frequency transmission was achieved with a 72 mm diameter quadrature resonator actively decoupled to a mouse quadrature surface coil used for reception (Bruker BioSpin, Ettlingen, Germany). A single slice (1 mm) flow-sensitive alternating inversion recovery (FAIR) sequence with a rapid acquisition with relaxation enhancement (RARE) readout was used (repetition time (TR)/recovery time/echo spacing (ΔTE)/effective echo time (TE_{eff}): 12 000/10 000/7.2/35.9 ms, respectively, 16 inversion times (35-1500 ms), RARE factor: 32, inversion slice thickness: 4 mm, 180° hyperbolic secant (sech80) inversion pulse (20 ms), field of view (FOV): 25.6 mm^2, matrix: 128 x 64 enlarged by partial fourier transform to 128 x 128, resolution: 200 μm^2, 12 min).

For angiography measurements, a 20 mm diameter quadrature volume coil (RAPID Biomedical, Rimpar, Germany) was used for radio frequency transmission and reception and a 3D time of light (TOF) sequence was used (TR/TE: 15/2.5 ms, α: 20 °, FOV: 25 mm^3, resolution: 98 x 130 x 196 μm^3 zero-filled to 98 μm^3, 6 min).

Spectroscopy, T_2 weighted and diffusion tensor imaging

T_2 weighted imaging, DTI, and MR spectra were acquired on a 7 T Biospec with a cryogenically cooled transmit/receive surface coil and Paravision 6.0 software (Bruker BioSpin, Ettlingen, Germany).

A 2D RARE T_2 sequence was used for anatomical images (TR/ΔTE/TE_{eff}: 3100/11/33 ms, RARE factor: 8, 29 consecutive slices, slice thickness 0.45 mm, FOV: $(16.2\ mm)^2$, resolution: 100 μm^2, NA: 2, 2 min 4 s). An isotropic echo planar imaging (EPI) DTI sequence was used (TR/TE: 7500/18 ms, 4 segments, 2 b values (0 and 1000 s/mm^2) with 5 b0 images, 126 gradient directions (1 experiment/direction), gradient duration (δ) 2.5 ms, gradient separation (Δ) 8.1 ms, 58 consecutive slices, FOV: 16.2 mm^2, acquisition matrix 72 x 48 enlarged by partial fourier transformation to 72 x 72, resolution: $(225\ \mu m)^3$, 1 h 5 min). Two animals, one from the sham and one from the hypoperfused group exhibited fluctuating respiration rates after the DTI

acquisition, did therefore did not undergo MRS (sham (n=8) and hypoperfused (n=10)) as. A stimulated echo acquisition mode (STEAM) sequence was used for spectroscopy following local shimming (MAPSHIM) across a cubic 8 mm^3 voxel placed in the striatum (TR/TE/mixing time: 2500 ms/3 ms/10 ms, number of averages (NA): 256, VAPOR water suppression, 10 min 40 s).

Data Analysis

Cerebral blood flow and angiography

CBF maps were calculated using the Perfusion ASL macro in Paravision 5.1 software via the T_1 method using a blood T_1 value of 2100 ms and a brain blood partition coefficient of 0.89 mL/g [1,2]. A custom written Matlab Release 2013a (MathWorks, Natick, MA, USA) script extracted the CBF maps from Paravision, and prompted manual delineation of regions of interest (ROI) in the striatum. The resulting CBF values were expressed in mL/min/100g.

Angiography images were analyzed as previously described [3]. Briefly, the spatial dimensions or the raw data was up-scaled by a factor of ten, exported into FSL software (Analysis Group, FMRIB, Oxford, UK), and the FLIRT tool was used for co-registration. Registered images were exported into ImageJ freeware (National Institutes of Health) and a maximum intensity projection (MIP) of the Circle of Willis was prepared with a custom plugin. A threshold (14 000 in 16 bit images, i.e. ~43% of max) was used to create a binary image of the MIP so that the number of voxels in the Circle of Willis could be counted and expressed in μm^2.

Spectroscopy and T_2 weighted imaging

MRS was analyzed using LCModel (version 6.3). Metabolite concentrations were calculated using water scaling to signal in a water-unsuppressed reference scan [4]. Data from one mouse in the sham and two mice in the hypoperfused group were excluded due to poor image and spectrum quality (sham (n=7) and hypoperfused (n=8)). Only values with an estimated standard deviation <25% were used for analysis. Due to this threshold, lactate was analyzed only for a subset of animals (sham (n=5) and hypoperfused (n=6)).

Ventricle to brain ratio (VBR) and hippocampal size were calculated from the T_2 weighted images. Outlines of all structures were manually delineated on a slice by slice basis in ImageJ, and total volumes of each were calculated by multiplying each area by slice thickness (0.45 mm) and summation.

Atlas registration and regional diffusion tensor imaging indices

Two animals, one from the sham and one from the hypoperfused group, were excluded from the analysis due to motion artifact that produced poor quality images (sham (n=9) and hypoperfused (n=10)). Quantitative DTI parameter maps (FA, mean, axial, and radial diffusivities (MD, AD, and RD, respectively) were calculated using Paravision 6. A mouse brain template (average of 12 different mouse brains), with a corresponding atlas containing masks of 23 different brain regions (modified from MRM NeAT Mouse Brain Database, Stony Brook, USA) [5] was co-registered to the data with a custom Matlab script, which first called the FSL FLIRT tool and second allowed for manual adaption of the transformation in order to improve the procedure. Both the template and the atlas were modified manually in ImageJ so that the structures better suited the FA maps in our group of animals. Furthermore, an additional 4 structures were added to the original atlas. A custom ImageJ macro extracted the DTI parameter values across all 23 different brain structures.

Tractography

Subsequent DTI data was analyzed in DSI Studio (http://dsi-studio.labsolver.org). First, tractography data were reconstructed with the DTI model. To select a white matter seed region, a whole brain mask (excluding ventricles) was extracted from the registered atlas. Background voxels with an FA value below 0.6 * the threshold determined by Otsu's method were excluded. Trajectories were subsequently calculated using a 4^{th} order Runge-Kutta method by placing $1 * 10^6$ seeds in the white matter volume (angular threshold 60°, step size half voxel size, minimum/maximum tract length 0.5 mm/20 mm, seed orientation "primary", seed position "subvoxel", no randomization of seeds, direction interpolation "trilinear").

Graph analysis

Graph analysis simplifies DTI data by constructing a graphical representation of nodes (brain structures) and edges (DTI trajectories connecting each structure) in order to obtain numerical values that represent certain network features. This process offers additional information regarding the brain as a whole, and represents an alternative to the qualitative representation of many individual fiber tracts. Adjacency matrices containing the weights of the edges were constructed in DSI Studio for each animal by counting the number of trajectories between the atlas brain structures (23 for each hemisphere). Only tracts that started in one and ended in another region were counted. Matrices were normalized by the total number of seeds and used to calculate graph metrics using the Brain Connectivity Toolbox [6] in Matlab.

Global efficiency is the average inverse shortest path length between all pairs of nodes. Modularity is a measure of the degree to which the overall network can be divided into distinct groups based on a maximum number of within group and minimum number of between group connections. Transitivity and clustering coefficient rely on the presence of triangles (groups of 3

connected nodes). Transitivity expresses the number of triangles as a ratio of the total number of connected triplets. If one particular node is connected to two neighbouring nodes, the clustering coefficient predicts the likelihood that the two neighbouring nodes are also connected and therefore represents the prevalence of clustering around individual nodes (averaged across all nodes). Local efficiency calculates the mean ability of sub-networks around nodes to exchange information when any given node is removed. No significant differences were noted between groups for degrees (a measure of centrality that calculates the average number of nodes that any given node shares a connection with) and assortativity (a measure of resilience that estimates a correlation between the degrees of all nodes on two opposing ends of the network)

Behavioural testing

Novel object recognition

NOR has been used to examine short term memory by taking advantage of the rodent's ability to recall features of objects presented a few hours prior; NOR was performed in accordance with a published protocol [7] except testing occurred in a standard mouse housing cage, and the objects were selected according to a different criterion. Different sets of wooden shapes were stored in bags filled with dirty bedding from animals within the same colony. Briefly, a camera was positioned over the test cage in a quiet room. Mice were habituated to the empty cage for 10 min on the day prior to testing. The following day two identical wooden objects were secured in an upright position to the floor of the cage equidistant from the edges. During the first trial, mice were placed inside the cage (snout facing away from the objects) and allowed to explore freely for 10 min. During the second trial (2 hrs later) the left object was replaced with another object of a different shape and smell, and mice were allowed to explore for 5 min. Videos were scored manually and the following parameters were recorded: total time spent with each object (s), total number of visits to each object, and latency to first contact each object (s). The discrimination ratio was calculated using the following formula (right object / (right object + left object)).

Water maze

A standard place task in the Morris water maze was used to assess spatial learning and reference memory [8]. Briefly, a circular maze (120 cm diameter) concealed a submerged escape platform with opaque water. Each animal received three daily trials over 7 consecutive days and the entry point to the pool was randomized with each trial. Trials were spaced approximately 20 min apart, and the animals were kept under a heat lamp in between. Each trial ended when the mouse located the platform, or, when the maximum time elapsed (90 s). Animals were collected approximately 10 s after locating the platform. In the case where the maximum time point was reached, animals were guided to the platform and made to wait for 10 s before collection. Escape latency (s), total distance travelled (cm), and swim speed (cm/s) were measured by a computerized tracking system (VideoMot, TSE Systems, Bad Homburg, Germany) and daily data was pooled. At 8 d, a probe trial was performed in which the platform was removed and the mice were allowed to swim for 90 s. The total time spent in the former target quadrant (s) was assessed.

Tissue preparation and staining procedures

At the conclusion of the experiments, mice were deeply anaesthetised and perfused through the heart with physiological saline followed by 4% paraformaldehyde. Subsequently, the brains were post-fixed for 24 hours, and cryoprotected in 30% sucrose solution before being snap frozen in -40 ºC methylbutane. Tissue was sectioned to 30 µm and stored in cryo-protective solution (1 part ethylene glycol, 1 part glycerine and 2 parts phosphate buffered saline (PBS)) at -20 ºC.

Immunohistochemistry

One series spanning the entire brain from each mouse was processed for standard diaminobenzidine (DAB) immunohistochemistry. Briefly, endogenous peroxidase activity was quenched (10% hydrogen peroxide (30%), 10% methanol, and 80% PBS) for 5 min and blocking was performed for 1 h in Triton-X PBS with 5% normal serum (Vector, Peterborough, UK). Tissue was rinsed extensively between steps with PBS. Sections were incubated with 1:2000 rabbit anti GFAP (Dako, Hamburg, Germany) and 1:500 rabbit anti Iba1 (Wako, Neuss, Germany) in Triton-X PBS overnight at 4 °C. The following day, the corresponding biotinylated secondary antibodies (1:100) were applied for 2 hours at room temperature, followed by a 1 h incubation in avidin and biotinylated horseradish peroxidase (Vectastain Elite ABC kit, Vector, Peterborough, UK). Visualization was performed with DAB (DAB Substrate kit, Vector, Peterborough, UK).

Luxol fast blue

One series spanning the entire brain from each mouse was mounted on slides and air-dried overnight. The following day, slides were placed in 70% ethanol for 30min followed by incubation in Luxol solution (2% in 96% ethanol with 0.5% acetic acid (10% stock solution)) at 60°C for 1:15 h. Sections were rinsed quickly in distilled water followed by a dip in 0.05% Li_2CO_3 to differentiate the white matter and a series of ethanol rinses (10 s in 95%, 1 min in 96%, and 30 s in 100%). Slides were cleared with Rotihistol and coverslipped with Vitro-Clud (R. Langenbrinck Labor und Medizintechnik, Emmendingen, Germany).

Statistical analysis

Normal distribution and homogeneity of variance were established with the Kolmogorov-Smirnov and Levine's tests, respectively, using SPSS Version 22 software (IBM, Hampshire, UK). CBF data, escape latencies in the water maze, and discrimination ratios in the NOR test were compared using a mixed design two way repeated measures ANOVA with surgery (sham versus microcoil) as the between subject factor, and time as the within subject factor. Performance in the water maze

probe trial, vascular size, VBR, and hippocampal size were compared between groups using an un-paired Student's t-test. Spectroscopy data, DTI parameter maps, and network analysis metrics were compared between groups using a series of un-paired Student's t-tests followed by a False Discovery Rate Control for multiple comparisons and Type I errors. All reported p values have been corrected. Correlations between performance in the water maze (area under the curve over the course of the 7 test days) and network analysis parameters were performed using Pearson's correlation. The logistic regression model for the graph theory data was performed in R Version 3.3 software (Free Software Foundation, R Foundation).

Supplemental figures and figure legends

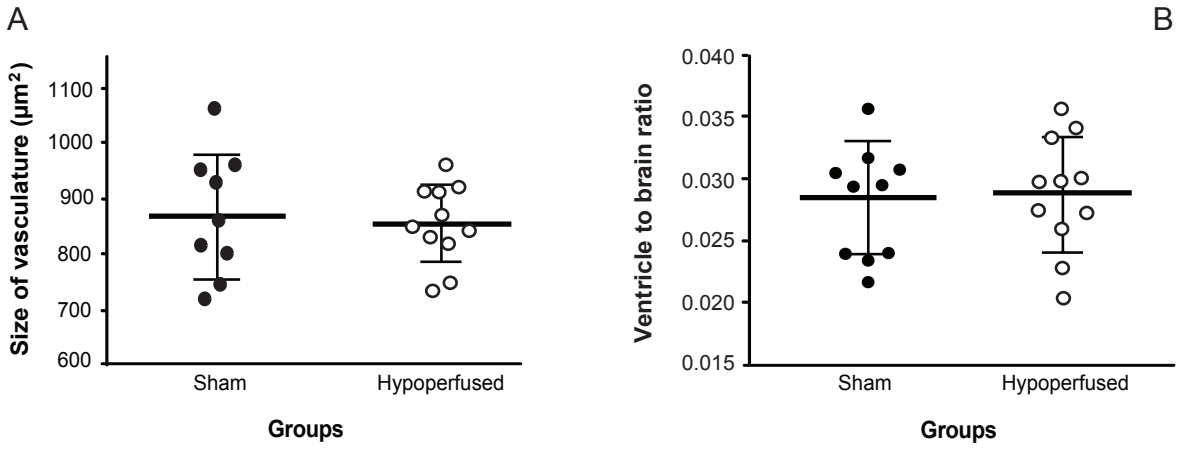

Figure I. Morphological changes in the hypoperfused brain. (A) Overall size of the Circle of Willis vasculature (means ± SD) in sham (n=10) and hypoperfused (n=11) groups, and (B) Ventricle to brain ratio (VBR).

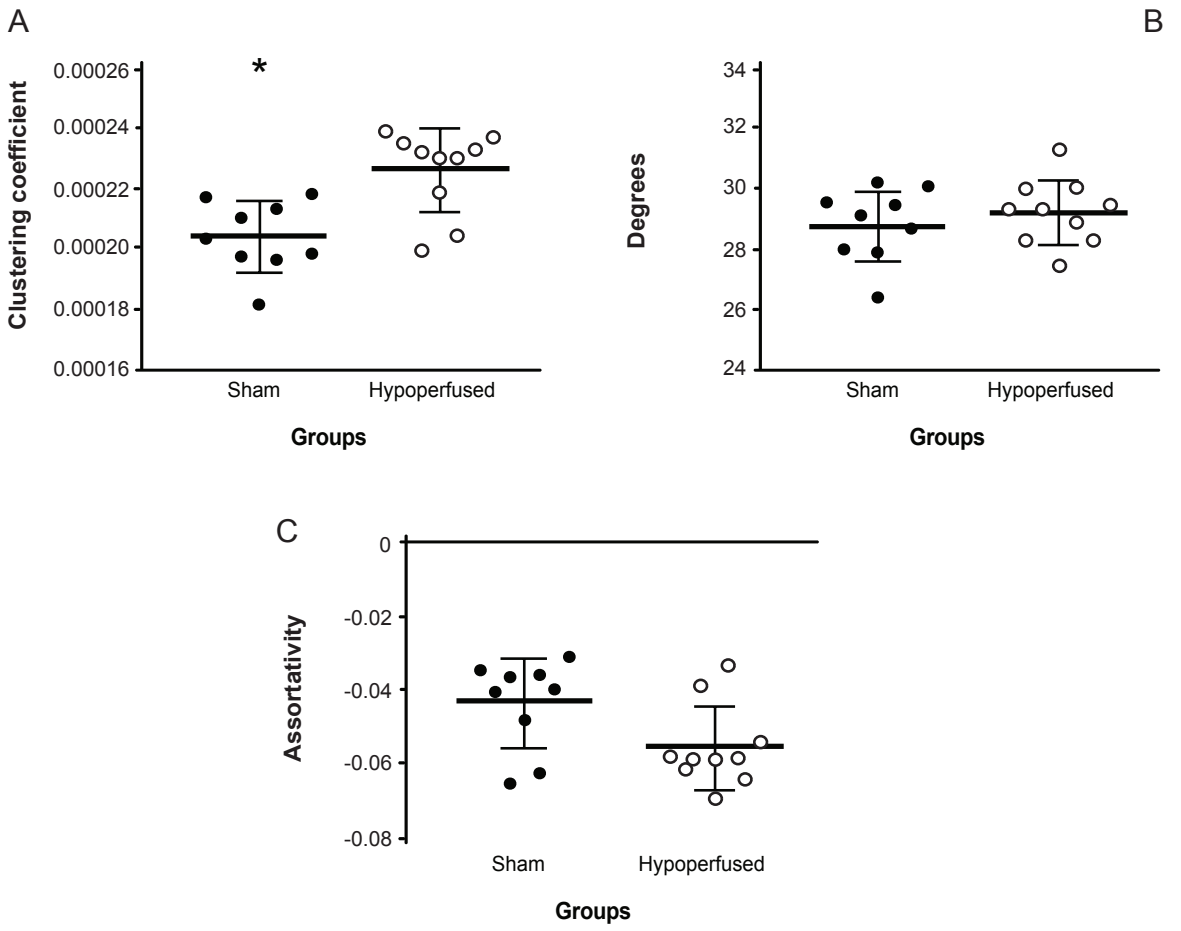

Figure II. Graph theory revealed microstructural network changes in the hypoperfused brain. (A) Clustering coefficient, (B) Degrees, and (C) Assortativity in both groups.

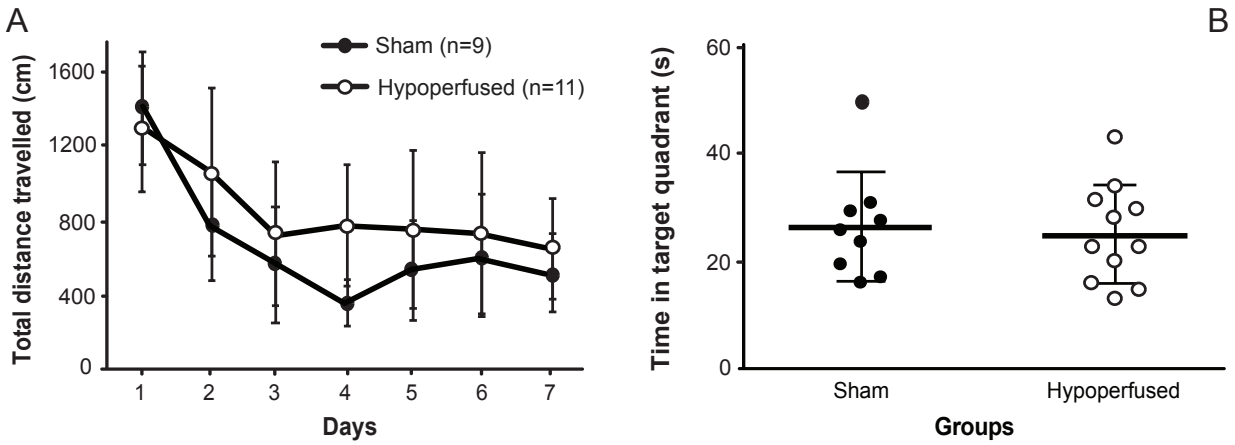

Figure III. The effects of hypoperfusion on distance travelled and reference memory in the Morris water maze. (A) Total distance travelled during the place task, and (B) time spent in the target quadrant during the probe trial (means ± SD).

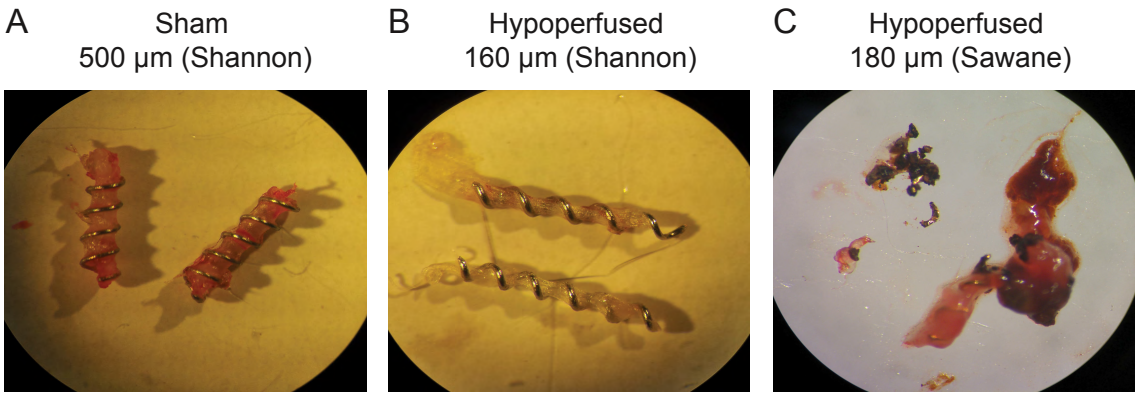

Figure IV. Microcoil manufacture influences material integrity. Photographs of microcoils harvested at the conclusion of the experiments from a sham (A) and hypoperfused (B) animal (500, and 160 µm diameter microcoils, respectively, Shannon, Coiled Springs Microcoil, Limerick, Ireland) show that the carotid arteries were still constricted at the end of the experiment in the hypoperfused group. Microcoils harvested from a hypoperfused animal (C) implanted with 180 µm diameter coils (from Sawane Spring Company, Hamamatsu, Japan) show substantial degradation after 1 month in the body.

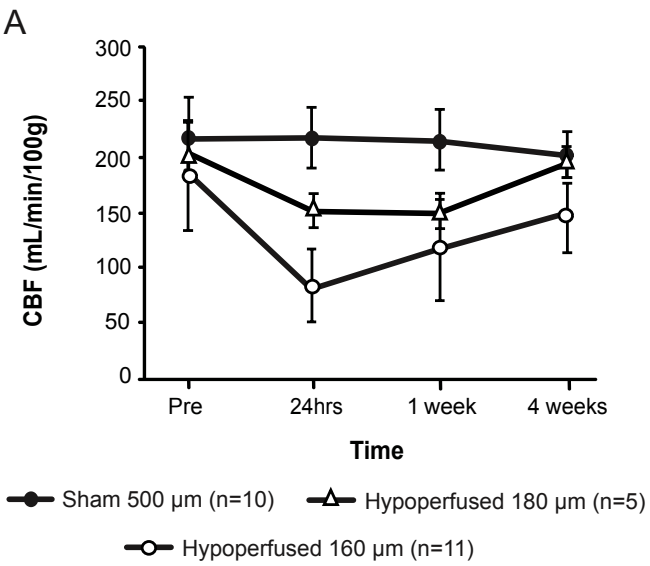

Figure V. Titrated cerebral blood flow (CBF) in the differentially hypoperfused brain. (A) CBF over time (means ± SD) in the sham (n=10) and hypoperfused (n=11) groups (500 and 160 µm diameter microcoils, respectively) with data superimposed from a group that was hypoperfused with standard 180 µm (n=5) diameter coils.

Supplemental References

1. Leithner C, Müller S, Füchtemeier M, Lindauer U, Dirnagl U, Royl G. Determination of the brain-blood partition coefficient for water in mice using MRI. *J. Cereb. Blood Flow Metab.* 2010;30:1821–4.
2. Dobre MC, Uğurbil K, Marjanska M. Determination of blood longitudinal relaxation time (T1) at high magnetic field strengths. *Magn. Reson. Imaging*. 2007;25:733–5.
3. Füchtemeier M, Brinckmann MP, Foddis M, Kunz A, Po C, Curato C, et al. Vascular change and opposing effects of the angiotensin type 2 receptor in a mouse model of vascular cognitive impairment. *J. Cereb. Blood Flow Metab.* 2015;35:476–484.
4. Provencher SW. Estimation of metabolite concentrations from localized in vivo proton NMR spectra. *Magn. Reson. Med.* 1993;30:672–9.
5. Ma Y, Smith D, Hof PR, Foerster B, Hamilton S, Blackband SJ, et al. In Vivo 3D Digital Atlas Database of the Adult C57BL/6J Mouse Brain by Magnetic Resonance Microscopy. *Front. Neuroanat.* 2008;2:1–10.
6. Rubinov M, Sporns O. Complex network measures of brain connectivity: Uses and interpretations. *Neuroimage*. 2010;52:1059–1069.
7. Bevins R a, Besheer J. Object recognition in rats and mice: a one-trial non-matching-to-sample learning task to study "recognition memory". *Nat. Protoc.* 2006;1:1306–11.
8. Vorhees C V, Williams MT. Morris water maze: procedures for assessing spatial and related forms of learning and memory. *Nat. Protoc.* 2006;1:848–58.